nature geoscience

ARTICLES
https://doi.org/10.1038/s41561-021-00827-9

Check for updates

Explosive or effusive style of volcanic eruption determined by magma storage conditions

Răzvan-Gabriel Popa[1]✉, Olivier Bachmann[1] and Christian Huber[2]

Most volcanoes erupt both effusively and explosively, with explosive behaviour being responsible for most human fatalities. Eruption style is thought to be strongly controlled by fast conduit processes, limiting our ability for prediction. Here we address a critical question in the quest to develop timely forecasting of eruptive behaviour: are there conditions in which the outcome of an eruption is predetermined by the state of the magma in the subvolcanic reservoir? We analyse the pre-eruptive storage conditions of 245 units from volcanoes around the world. We show that pre-eruptive crystallinity, dissolved water content and the presence of exsolved volatiles in the chamber exert a primary control on eruptive styles. Magmas erupt explosively over a well-defined range in dissolved water content (~4–5.5 wt%) and crystallinity (less than 30 vol%). All other conditions, namely higher crystallinity, dissolved water contents below 3.5 wt% and, counterintuitively, in excess of 5.5 wt%, favour effusive activity. Between these ranges, there is a narrow field of transitional storage properties that do not discriminate between eruptive styles, and where the conduit exerts the main control on eruptive behaviour. Our findings suggest that better estimates of crystallinity and water content in subvolcanic chambers are key to forecasting eruptive style.

Volcanic eruptions often lead to fatalities, but explosive behaviour on its own accounts for more than 95% of human casualties[1]. In light of this, over the past decades, the scientific community has made substantial progress in unravelling how syneruptive and conduit processes influence the eruptive behaviour of volcanoes[2–22]. To a first order, eruptive style is thought to depend dominantly on conduit processes, namely on whether the gas remains trapped in the magma or escapes and outgases during ascent[3]. In the first case, the trapped gas bubbles expand, accelerate and fragment the magma column, releasing the energy required for explosive activity. In the second case, outgassing neutralizes the explosive potential of the magma, resulting in effusive eruptions. However, most volcanoes are known to manifest both effusive and explosive behaviour, sometimes simultaneously[10,23], and a clear understanding of the factors that control transitions between effusive and explosive eruptions remains elusive.

In this study, we focus on the question: are there conditions on the state of the magma stored before an eruption that predetermine whether the next event will be effusive or explosive? If so, what are the parameters that one should constrain? Can the same conceptual framework explain the common occurrence of effusive precursors observed at the onset of highly explosive events, including caldera collapses (for example, volcan Quizapu[24], Quilotoa volcano[15], Mount Pinatubo[25], the Fish Canyon Tuff sequence[26] or sequences of the Aira caldera[27])?

To analyse the role that various pre-eruptive parameters have on eruption behaviour, we perform a survey of the pre-eruptive magma chamber conditions that were prevalent when effusive and explosive eruptions initiated at various volcanoes around the globe (Fig. 1). We have mostly considered arc volcanoes, which generally show highly variable volatile contents, favouring a broad range of eruptive styles. We have selected volcanic eruptions involving intermediate to silicic magmas (andesites to rhyolites), which are expected to have broadly similar rhyodacitic to rhyolitic melts, and inherently comparable compositional effects on viscosity and water saturation levels. For representability, we selected volcanoes with subvolcanic storage regions located at around 2 kbar, which is the most common pressure for upper-crustal magmatic storage in such settings[28]. We restrict the storage pressure to avoid variations in the water saturation level caused by this parameter.

Rationale and investigated parameters

We reconstruct a snapshot of the pre-eruptive conditions for 245 eruptive events, based on previously published data (Supplementary Data 1). Our goal is to evaluate pre-eruptive (1) storage temperatures, (2) dissolved water contents and (3) crystallinities. We correlate these properties with eruptive styles (here categorized as effusive or explosive) and with the potential pre-eruptive presence of a water-dominated magmatic volatile phase (exsolved 'gas'), to highlight their effect on effusive–explosive transitions. In some instances, specifically when both types of eruption occurred simultaneously, defining an eruption style might be ambiguous. In the case of contemporaneous eruptions, we make this distinction based on the style of eruption that initiated the event, and for older eruptions based on the type of deposit that was analysed. In the special case of dome or sector collapse events, the eruptive style is still considered effusive because the explosion is a secondary surface effect caused by gravitational processes.

Storage temperature is defined here as the temperature of the eruptible batch of magma before eruption triggering. This is an essential parameter that constrains the dissolved water content and the water saturation level of the melt. To avoid the potential reheating effect of mafic recharge, which is one of the most common processes leading to eruptions[29], we consider the pre-recharge, pre-reheating temperature recorded by minerals crystallized in the subvolcanic reservoir. As a first choice, we applied the amphibole-plagioclase thermometer[30], which we used throughout the dataset for consistency. Where amphibole did not crystallize in equilibrium with the pre-eruptive mineral assemblage, we relied on the pyroxene thermometers[31]. We would like to stress that Fe-Ti oxides, used

[1]Institute of Geochemistry and Petrology, ETH Zürich, Zürich, Switzerland. [2]Department of Earth, Environmental & Planetary Sciences, Brown University, Providence, RI, USA. ✉e-mail: razvan.popa@erdw.ethz.ch

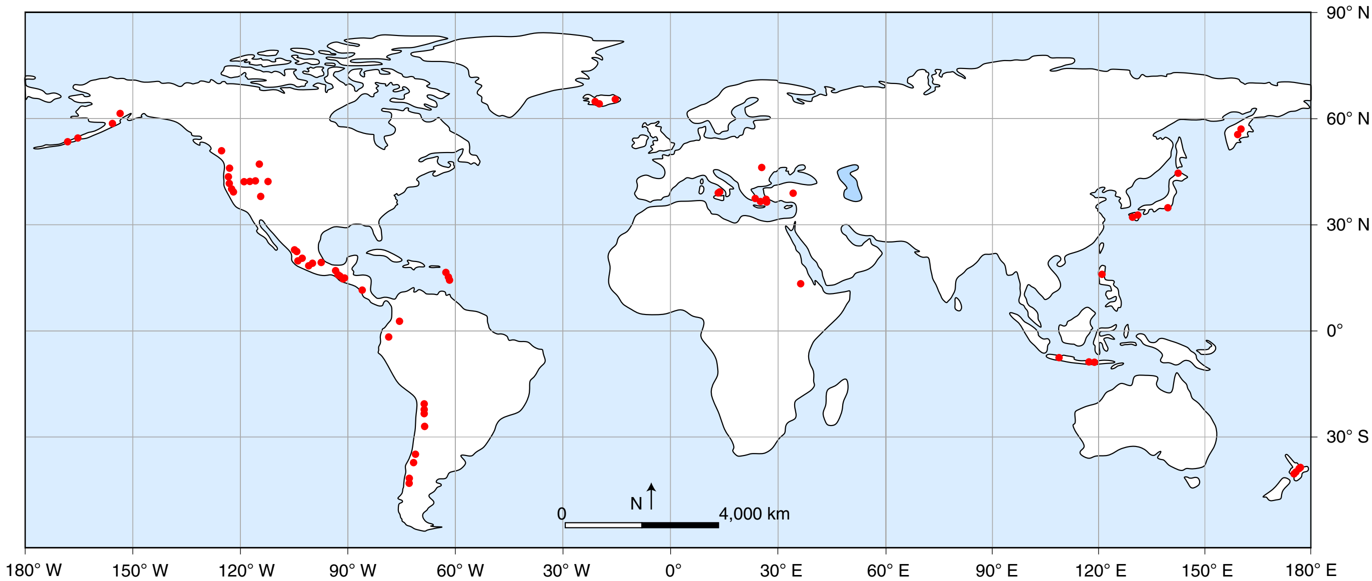

Fig. 1 | World map showing the location of the volcanoes considered in this study. We have analysed a total of 245 eruptions, 133 effusive and 112 explosive, from 75 different volcanoes or volcanic areas. These include famous volcanoes such as Crater Lake, Santorini, Nisyros, Pinatubo, Unzen and others. The complete list of eruptive events, the data and the references are available in Supplementary Data 1.

extensively in thermometric estimates, re-equilibrate in a matter of hours to days to fluctuating temperatures[32]. This makes Fe-Ti oxide thermometry unlikely to record accurate storage temperatures whenever extensive reheating occurred before eruptions, as is the case with many effusive events[24,33,34]. Hence Fe-Ti oxide thermometry is more likely to record post-recharge eruptive temperatures[24,35], and should be used with care when estimating storage temperatures.

Dissolved water content in magmas is generally one of the most difficult parameters to determine. Direct measurements of water in melt inclusions are often biased by the diffusive loss during the slow-cooling regimes experienced by lava flows[36,37]. This makes the comparison between the volatile budgets of effusive and explosive deposits unreliable[35]. To overcome this caveat, we rely on formulations of mineral-melt equilibria, by applying the same plagioclase-melt hygrometer[38] throughout the dataset. The inputs used are the compositions of the plagioclase rims, groundmass glass or melt-inclusion composition and storage temperature. When available, direct estimates of dissolved water contents based on melt-inclusion measurements are used for explosive deposits, where the fast quenching of the tephra preserves initial water contents.

Crystallinity is defined here as the volume% of phenocrysts. It reflects the crystallinity of the magma at the onset of eruption. Microlites tend to form during the undercooling of the magmas, during slow conduit ascent and post-emplacement, and are hence excluded.

Considering these, our ability to reconstruct the magmatic pre-eruptive conditions is limited by the availability of published data for a given eruption. For each of the eruptive events included in the analysis we ideally require the following: crystallinity estimates, plagioclase rim compositions, amphibole or pyroxene rim compositions, groundmass glass or melt-inclusion compositions, or direct estimates of dissolved water contents from melt inclusions (reliable for explosive deposits). Although considerably more eruptive events are described in the literature, we generally discard events for which a complete dataset is lacking. Exceptions are some units where, in the absence of mineral data required for thermometry, we use experimental constraints on storage temperature instead. We also include a few eruptions despite lacking storage temperature data, with the condition that water-content estimates through direct

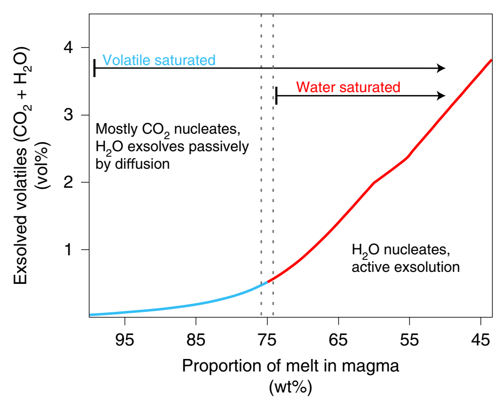

Fig. 2 | Plot depicting the increase in the volume of exsolved volatiles (CO_2+H_2O) with crystallization. The calculations are made for storage of a rhyolitic magma at a pressure of 2 kbar. The exsolution is modelled using rhyolite-MELTS[40], starting from the composition of the Nikia lava flow from Nisyros volcano[35], with an initial 4.5 wt% of dissolved H_2O and 500 ppm CO_2, as it cools from 950 °C to 730 °C. Blue indicates the increase in exsolved volatiles during water-undersaturated differentiation, while red depicts the same for water-saturated crystallization. The dashed lines mark the moment of water saturation.

measurements are available (that is, the analysis does not require hygrometry calculations).

In light of the effect it has on eruption dynamics, the physical state of the volatiles is yet another parameter that we need to consider. Volatiles (that is, H_2O, CO_2, Cl, S) can be found both in a dissolved state (molecularly disseminated in the melt) and in an exsolved state ('vapour', or more precisely magmatic volatile phase, MVP)[39]. Once a volatile species reaches its saturation limit in the melt, exsolution is favoured. However, it is when the most abundant volatile (that is, H_2O) reaches saturation that the volume fraction of MVP increases substantially. This is illustrated in Fig. 2, based on rhyolite-MELTS simulations[40]. Hence, it is important to note the difference between

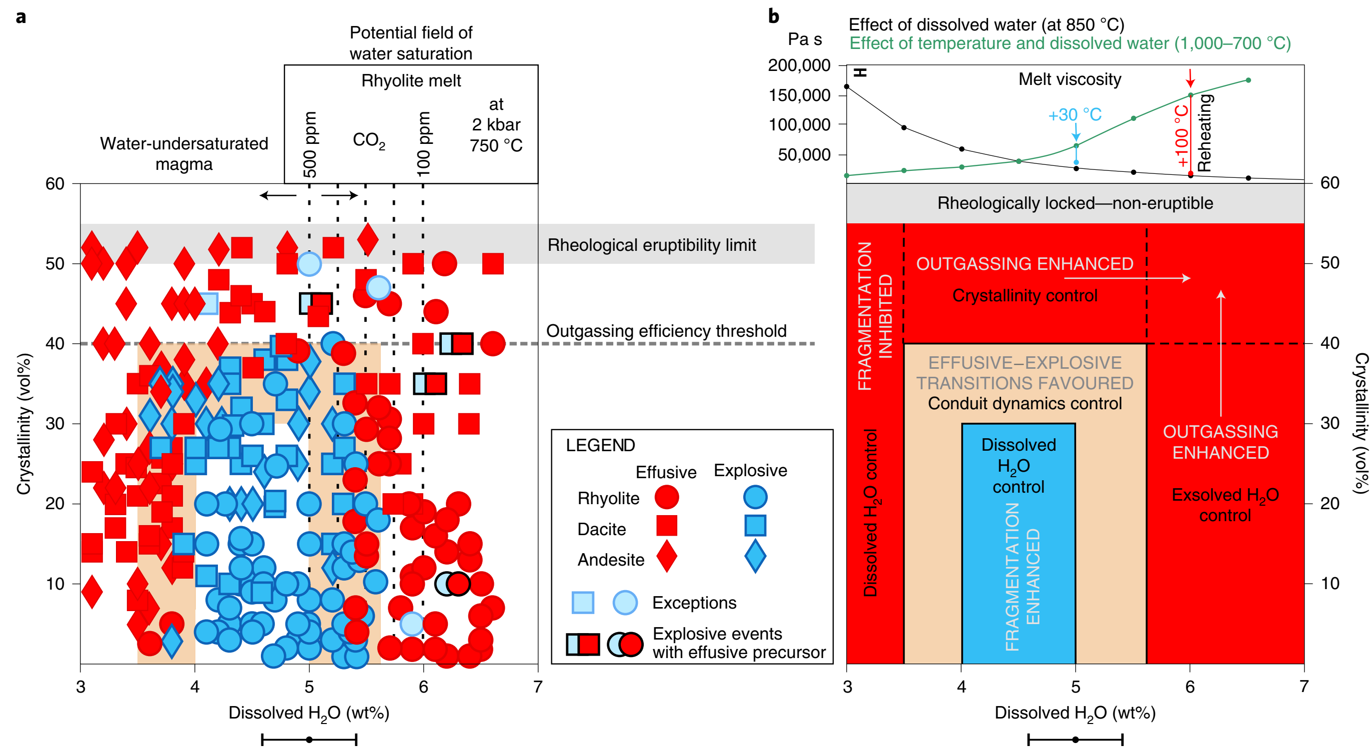

Fig. 3 | Correlation of eruptive styles with crystallinity, dissolved H_2O and water saturation. a,b, The data (**a**) and the results translated into a regime diagram (**b**). The potential field of water saturation is calculated for a magma with rhyolitic melt stored at 2 kbar (ref. [44]). For illustrative purposes, we use a temperature of 750 °C and varying CO_2 concentrations (vertical dashed lines in **a**). The data show a clear window of explosivity separated from the effusive domain by a transitional field (orange background). In the transitional field, water content and crystallinity fail to discriminate between effusive and explosive eruptions. According to the data, this corresponds to magmatic conditions at which both eruptive styles are possible and the ensuing eruptive behaviour is likely to be dominantly controlled by the conduit dynamics. Outside this field, the magmatic properties inherited from the magma chamber predetermine the eruptive behaviour. The crystallinity threshold at which permeable outgassing is favoured[51] and the rheological eruptibility limit[59] are also depicted. Above the regime diagram, the evolution of melt viscosity[54] with (1) increasing dissolved water at constant temperature (black curve, 850 °C) and (2) the combined effect of increasing dissolved water and magmatic cooling (green curve) is depicted. For the viscosity calculation, the thermal and water-content evolution is modelled using rhyolite-MELTS[40], starting from a dacitic composition at 3 wt% dissolved water over a cooling range from 1,000–700 °C. The water-undersaturated and saturated melts are reheated by 30 °C (at 5 wt% H_2O) and 100 °C (at 6 wt% H_2O) to test the effect that hot recharge has upon eruptive melt viscosity for a Nisyros-type explosive (blue line) and effusive case (red line)[35]. For the uncertainty calculation on dissolved H_2O, we use the average relative errors of the storage temperature and the uncertainty of the hygrometer, which we propagate in quadrature. The average propagated error of the dissolved water content over the interval analysed is 9.2% relative, which translates to the average absolute error of ±0.41 wt% H_2O.

volatile saturation, which will probably start with the exsolution of MVPs dominated by CO_2 and S, and water saturation, which will occur later during the differentiation of the melt. It has recently been shown through numerical modelling[34,41,42] and supported by studies on natural volcanic samples[35,43] that exsolved volatiles increase the compressibility of the magma in the reservoir. Increased compressibility allows for greater mass of hot recharge to be accommodated in the subvolcanic magma chamber before the eruption initiates, thereby leading to magma reaching a higher temperature before eruption. This influences the melt rheology and the ability of the MVP to outgas during ascent. Based on Fig. 2, the mechanical effect that exsolved volatiles have on the magma chamber is greater once the melt differentiates beyond water saturation. Hence, the distinction between water-undersaturated and water-saturated environments is relevant to our analysis and is used henceforth.

The correlation between magma chamber and eruptive styles

In a water-undersaturated environment, pre-eruptive dissolved water content and crystallinity correlate with eruptive behaviour (Fig. 3). Overall, it appears that dissolved water contents of <3.5 wt% are insufficient to yield explosive eruptions in andesites to rhyolite. On the other hand, there is a window of water content between ~4 to 5.5 wt% for magmas with crystallinity <30 vol%, where eruptions are dominantly explosive (Figs. 3, 4a). The upper limit of 5.5 wt% corresponds to the water saturation limit of the melt and can show some variability, most likely because of the effect of CO_2 and storage temperature on water solubility[44]. Notably, magmas with a pre-eruptive crystallinity in excess of ~40 vol% erupt mostly effusively, irrespective to the water content. Lastly, the data clearly show that magmas with as much as 5.5–6.5 wt% dissolved H_2O are, counterintuitively, prone to erupt effusively. For the storage pressure and compositions considered here, these high dissolved water contents probably reflect saturation levels and the water-rich effusive magmas were probably stored in the presence of exsolved water in the subvolcanic reservoir (the 'excess' exsolved water is not recorded by hygrometry) (Fig. 3).

The different regimes outlined above can all be explained in light of a 'fragmentation potential', where fragmentation is promoted by the build-up of large stresses (or strain-rate)[45] that cannot be accommodated by deformation of the magma as it rises to the surface[3]. Large stresses are generated by bubble overpressure in a decompressing magma[46] or by shear deformation along conduit walls in a rapidly ascending magma[14,47]. Under both conditions, efficient

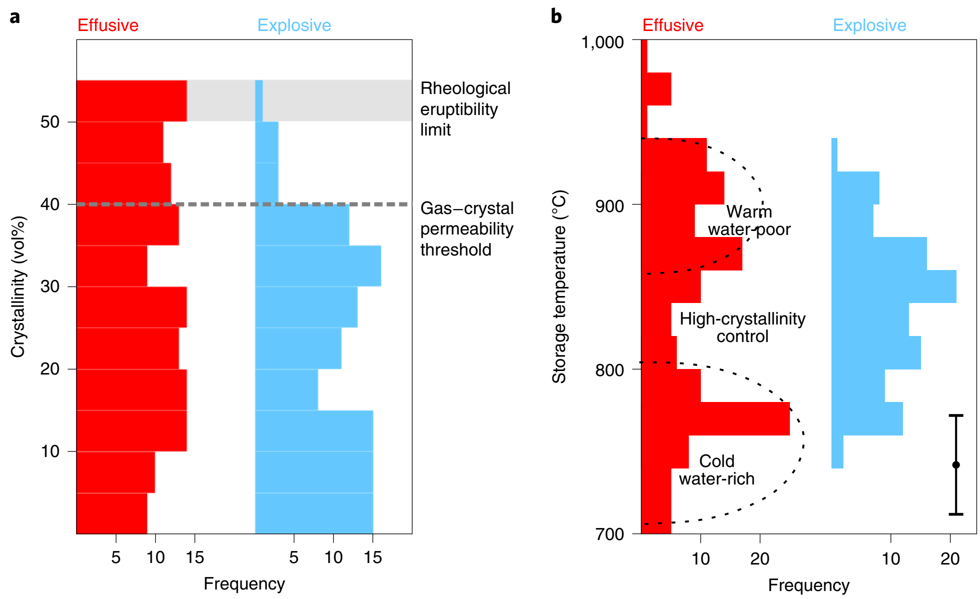

Fig. 4 | The distribution of crystallinity and storage temperatures with eruptive behaviours. a,b, Histograms showing the distribution of crystallinity (**a**) and storage temperatures (**b**) with eruptive behaviours. The frequency of explosive events decreases drastically at crystallinities >40 vol% (horizontal dashed grey line in **a**), while effusive events occur over the entire crystallinity range (0–55 vol%). Magmas behaving explosively seem to be stored in a relatively well-constrained interval of temperatures, roughly between 770 and 900 °C with a maximum frequency between 800 and 880 °C. Effusive events occur over a larger interval of storage temperatures (700–1,000 °C), with maximum frequency at <800 °C (colder temperatures characteristic of differentiated magmas at water saturation) and >850 °C (warmer temperatures favouring lower melt viscosities and gas permeability development[24]) (areas enclosed by black dashed lines in **b**).

outgassing reduces magma buoyancy and ascent rate and limits the potential for fragmentation.

The data from the 245 events support that a high fragmentation potential is mostly found over a limited but well-defined range of conditions: low crystallinity (<30 vol%) and water-undersaturated melt with dissolved water content between ~4–5.5 wt%. On the other hand, fragmentation seems unlikely to occur at dissolved water contents of <3.5 wt%, unless external triggers are involved (hydromagmatic interactions[22] or sector collapse[48]) or unless the CO_2 content of the melt is high (which has been shown to reduce pore interconnectivity and promote fragmentation[49]). A potential explanation deserving further thought is that melts with lower dissolved water contents saturate at shallower levels in the conduit. In this case, the gas bubbles are subjected to smaller amounts of decompression, limiting their ability to over-pressurize the melt beyond the glass transition and hence to accelerate and fragment the magma before reaching the surface. This may cause the low-water-content systems to have a low fragmentation potential. The effusive behaviour of the high crystallinity magmas (>40 vol%) is probably caused by efficient outgassing through porous networks of crystals[50–52] during ascent. Outgassing of crystal-rich magma is additionally promoted by its higher bulk viscosity, which limits the ascent velocity and allows additional time for the gas bubbles to escape the melt[53], rather than fragment it.

Finally, the dominantly effusive eruptions of magmas with ~5.5–6.5 wt% dissolved water could potentially be explained through three combined effects. First, the solubility of water in the melt depends strongly on CO_2 content and storage temperature[44]. For example, for storage temperatures of ~750 °C and pressures of ~2 kbar, water solubility can range from 5 wt% H_2O at 500 ppm CO_2 to >6 wt% H_2O at <100 ppm CO_2 (ref. [44]). Our dataset indicates that most arc magmas tend to saturate with water at >5.5 wt% H_2O, so this value can be taken as a crude reference. This generally coincides to storage temperatures of <780 °C, where effusive events become more frequent (Fig. 4b). In water-saturated systems, a notable increase in the bubble volume fraction present in the storage chamber is expected. These vapour bubbles increase the magma compressibility (Fig. 5a) and therefore enhance the thermal response of the magma to recharges (Fig. 5c, higher temperature increase)[24,34,35]. It results in decreasing the melt viscosity of the magma immediately before its ascent, favouring gas mobility and reducing the build-up of the large stresses required to initiate fragmentation. Second, the high dissolved water content also reduces the melt viscosity[54] (Fig. 3b) and therefore the magnitude of the stresses imposed on the magma during ascent. Furthermore, since the amount of water dissolved in the melt is effectively buffered at water-saturated levels, the melt contains the maximum dissolved water content possible for the given storage pressure, which maximizes its potential effect on decreasing melt viscosity[54]. Third, the existence of exsolved volatiles at the onset of or early during conduit ascent could enhance early, deep outgassing and provides additional gas nucleation sites for the already saturated magma[35,43]. Hence, hydrodynamic interactions between bubbles, including coalescence, are likely to start deeper in the conduit for magmas that are stored under water-saturated conditions (similar vesicularity reached ~2 km deeper compared with water-undersaturated melts with 4.5 wt% dissolved water[43]). Notably, this effect occurs under thermal and rheological conditions (first and second points above) that are more favourable to allow outgassing than in the water-undersaturated case.

As a note related to the effect of exsolved volatiles in the mechanical and thermal response of magma chambers to recharges (Fig. 5), it can occur regardless of magma chamber volume, as long as the response of the host crust is dominantly elastic and the rate of cooling of the magma is lower than the rate of pressurization caused by recharge[55]. We expect this behaviour to prevail for most upper-crustal subvolcanic magmatic reservoirs, with a qualitatively similar trend, albeit with different amplitude when considering

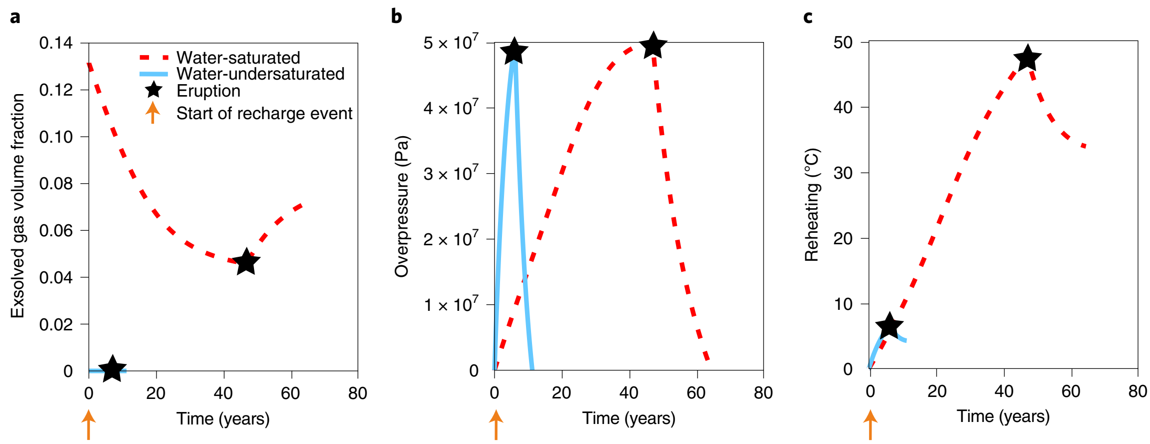

Fig. 5 | Response of reservoirs containing water-saturated and water-undersaturated magmas to recharge events. The results are derived from running a new simulation with a published numerical model[34,56] for the typical case of effusive and explosive eruptions at Nisyros volcano. The maximum overpressure required to initiate an eruption is set to 50 MPa. The size of the reservoir (30 km^3), the temperature of recharge (950 °C) and the recharge rate over time (0.1 km^3 yr^{-1}) are the same between the two examples and are kept constant. The water-undersaturated magma has a pre-recharge storage temperature of 820 °C, while the water-saturated magma has a colder storage temperature of 750 °C and an initial volume of exsolved gas >10%. **a**, The decrease in the volume fraction of exsolved gas in response to the influx of mafic recharge, caused by the compressibility of the exsolved gas and, to some degree, by re-dissolution due to pressure increase. **b**, All else being equal, the existence of a compressible exsolved volatile phase requires a greater amount of mass injected in the chamber to reach the critical overpressure that initiates the eruption. At a constant recharge rate, this translates into longer recharge times. **c**, The compressibility–reheating feedback, with the water-saturated reservoir being subjected to greater volumes of hot recharge over a longer time period, resulting in a greater temperature increase.

different chamber volumes. Deviation in storage pressure within the average uncertainty of our estimations (2 ± 0.5 kbar) does not affect the critical overpressure substantially, which is mostly controlled by the yield strength of the surrounding rocks[56]. Larger magma chambers will, however, require longer times of recharge, or higher fluxes of recharge to reach the point of eruption triggering.

Additionally, the data show three narrow domains in crystallinity:dissolved-water-content space where both effusive and explosive events co-exist (Fig. 3). These three narrow domains frame the explosivity window and indicate the conditions where magmatic storage properties do not discriminate between eruptive behaviours. These domains reflect the magmatic conditions where conduit processes are likely to decide whether an eruption will behave effusively or explosively. They might describe the range of magmatic properties for which effusive–explosive transitions can occur during the same eruption, or even simultaneously, generating hybrid events[10,23].

We also observe some notable exceptions to the trends discussed above: for example, the occurrence of explosive eruptions of calc-alkaline magmas that were potentially water-saturated, or that were crystal-rich (Fig. 3, light blue). There are several possible explanations. First, the exceptions we have identified are generally related to caldera-forming events, where roof collapse is expected to induce extreme rates of material evacuation. Such rates are fast enough to overwhelm outgassing even if the latter is promoted by high crystallinity. Second, we note that many of the explosive exceptions, either caldera-forming or not, were preceded by effusive precursors (for example, volcan Quizapu[24], Mount Pinatubo[23], Quilotoa volcano[15] and so on). The effusive precursors respect the general trends we have identified. However, the 'opening' of the magmatic reservoir that is associated with the precursory eruption can lead to its partial open-system outgassing, which might deplete the exsolved water. This effectively keeps the system at water saturation, but with a low volume of MVP remaining at subvolcanic storage, insufficient to generate the compressibility–reheating-permeability development feedback. Therefore, by removing the excess exsolved volatiles, an effusive eruption can prime the magmatic system for a highly explosive event. This will depend on the effused volume, on the duration of the precursory eruption and on the size of the magma chamber[34,57]. A third type of exception is when magmas of 'low fragmentation potential' interact with non-magmatic water, as is the case of eruptions occurring in lakes (for example, Taupo or Okataina volcanic centres). In this situation, an initial hydromagmatic fragmentation event can generate a decompression wave through the magmatic column and cause an explosive eruption. Last, dome collapses and/or volcanic landslides can send fast decompression waves into the shallow part of the plumbing systems and trigger explosive events, despite magma chamber conditions being favourable to effusive behaviour (for example, Mount St. Helens, 1980)[48].

Under most circumstances, notably in the absence of external drivers, our analysis shows that whether an eruption will behave effusively or explosively is, to a large extent, predetermined by the state of the magma in the shallow subvolcanic storage region. The main parameters to consider are pre-eruptive crystallinity, dissolved water content and the water saturation state of the melt, which require the pre-eruptive temperatures to be determined as well. Better estimates of these parameters at active volcanoes would improve our ability to predict the behaviour of a forthcoming eruption, especially if combined with geophysical tools that have the potential for estimating crystallinity and identifying the presence of substantial volume fractions of MVPs (for example, magnetotelluric imaging surveys[58]).

Online content

Any methods, additional references, Nature Research reporting summaries, source data, extended data, supplementary information, acknowledgements, peer review information; details of author contributions and competing interests; and statements of data and code availability are available at https://doi.org/10.1038/s41561-021-00827-9.

Received: 3 November 2020; Accepted: 22 August 2021;
Published online: 30 September 2021

References

1. Brown, S. K., Jenkins, S. F., Sparks, R. S. J., Odbert, H. & Auker, M. R. Volcanic fatalities database: analysis of volcanic threats with distance and victim classification. *J. Appl. Volcanol.* **6**, 15 (2017).
2. Cassidy, M., Manga, M., Cashman, K. & Bachmann, O. Controls on explosive-effusive volcanic eruption styles. *Nat. Commun.* **9**, 2839 (2018).
3. Gonnermann, H. M. & Manga, M. The fluid mechanics inside a volcano. *Annu. Rev. Fluid Mech.* **39**, 321–356 (2007).
4. Eichelberger, J. C., Carrigan, C. R., Westrich, H. R. & Price, R. H. Non-explosive silicic volcanism. *Nature* **323**, 598–602 (1986).
5. Papale, P. Dynamics of magma flow in volcanic conduits with variable fragmentation efficiency and nonequilibrium pumice degassing. *J. Geophys. Res. Solid Earth* **106**, 11043–11065 (2001).
6. Ripepe, M. et al. Effusive to explosive transition during the 2003 eruption of Stromboli volcano. *Geology* **33**, 341–344 (2005).
7. Melnik, O., Barmin, A. A. & Sparks, R. S. J. Dynamics of magma flow inside volcanic conduits with bubble overpressure buildup and gas loss through permeable magma. *J. Volcanol. Geotherm. Res.* **143**, 53–68 (2005).
8. Adams, N. K., Houghton, B. F. & Fagents, S. A. The transition from explosive to effusive eruption regime: the example of the 1912 Novarupta eruption, Alaska. *Geol. Soc. Am. Bull.* **118**, 620–634 (2006).
9. Cabrera, A., Weinberg, R. F., Wright, H. M. N., Zlotnik, S. & Cas, R. A. F. Melt fracturing and healing: a mechanism for degassing of silicic obsidian. *Geology* **39**, 67–70 (2011).
10. Castro, J. M. et al. The role of melt-fracture degassing in defusing explosive rhyolite eruptions at volcán Chaitén. *Earth Planet. Sci. Lett.* **333-334**, 63–69 (2012).
11. Nguyen, C. T., Gonnermann, H. M. & Houghton, B. F. Explosive to effusive transition during the largest volcanic eruption of the 20th century (Novarupta 1912, Alaska). *Geology* **42**, 703–706 (2014).
12. Preece, K. et al. Transitions between explosive and effusive phases during the cataclysmic 2010 eruption of Merapi volcano, Java, Indonesia. *Bull. Volcanol.* **78**, 54 (2016).
13. Dingwell, D. B. Volcanic dilemma: flow or blow? *Science* **273**, 1054–1055 (1996).
14. Papale, P. Strain-induced magma fragmentation in explosive eruptions. *Nature* **397**, 425–428 (1999).
15. Rosi, M., Landi, P., Polacci, M., Di Muro, A. & Zandomeneghi, D. Role of conduit shear on ascent of the crystal-rich magma feeding the 800-year-b.p. Plinian eruption of Quilotoa volcano (Ecuador). *Bull. Volcanol.* **66**, 307–321 (2004).
16. Mastin, L. G. The controlling effect of viscous dissipation on magma flow in silicic conduits. *J. Volcanol. Geotherm. Res.* **143**, 17–28 (2005).
17. Burgisser, A. & Gardner, J. E. Experimental constraints on degassing and permeability in volcanic conduit flow. *Bull. Volcanol.* **67**, 42–56 (2005).
18. Castro, J. M. & Gardner, J. E. Did magma ascent rate control the explosive–effusive transition at the Inyo volcanic chain, California? *Geology* **36**, 279–282 (2008).
19. Degruyter, W., Bachmann, O. & Burgisser, A. Controls on magma permeability in the volcanic conduit during the climactic phase of the Kos Plateau Tuff eruption (Aegean Arc). *Bull. Volcanol.* **72**, 63–74 (2010).
20. Mader, H. M., Llewellin, E. W. & Mueller, S. P. The rheology of two-phase magmas: a review and analysis. *J. Volcanol. Geotherm. Res.* **257**, 135–158 (2013).
21. Pollaci, M., Rosi, M., Landi, P., Di Muro, A. & Papale, P. Novel interpretation for shift between eruptive styles in some volcanoes. *Eos* **86**, 333–340 (2005).
22. Parfitt, E. A. & Wilson, L. *Fundamentals of Physical Volcanology* (Blackwell, 2008).
23. Wadsworth, F. B., Llewellin, E. W., Vasseur, J., Gardner, J. E. & Tuffen, H. Explosive–effusive volcanic eruption transitions caused by sintering. *Sci. Adv.* **6**, eaba7940 (2020).
24. Ruprecht, P. & Bachmann, O. Pre-eruptive reheating during magma mixing at Quizapu volcano and the implications for the explosiveness of silicic arc volcanoes. *Geology* **38**, 919–922 (2010).
25. Pallister, J. S., Hoblitt, R. P. & Reyes, A. G. A basalt trigger for the 1991 eruptions of Pinatubo volcano? *Nature* **356**, 426–428 (1992).
26. Bachmann, O., Dungan, M. A. & Lipman, P. W. Voluminous lava-like precursor to a major ash-flow tuff: low-column pyroclastic eruption of the Pagosa Peak Dacite, San Juan volcanic field, Colorado. *J. Volcanol. Geotherm. Res.* **98**, 153–171 (2000).
27. Geshi, N., Yamada, I., Matsumoto, K., Nishihara, A. & Miyagi, I. Accumulation of rhyolite magma and triggers for a caldera-forming eruption of the Aira Caldera, Japan. *Bull. Volcanol.* **82**, 44 (2020).
28. Huber, C., Townsend, M., Degruyter, W. & Bachmann, O. Optimal depth of subvolcanic magma chamber growth controlled by volatiles and crust rheology. *Nat. Geosci.* **12**, 762–768 (2019).
29. Bachmann, O. & Huber, C. Silicic magma reservoirs in the Earth's crust. *Am. Mineral.* **101**, 2377–2404 (2016).
30. Holland, T. & Blundy, J. Non-ideal interactions in calcic amphiboles and their bearing on amphibole-plagioclase thermometry. *Contrib. Mineral. Petrol.* **116**, 433–447 (1994).
31. Putirka, K. in *Minerals, Inclusions and Volcanic Processes; Reviews in Mineralogy and Geochemistry* Vol. 69 (eds Putirka, K. & Tepley, F.) 61–120 (Mineralogical Society of America, 2008).
32. Venezky, D. & Rutherford, M. Petrology and Fe-Ti oxide reequilibration of the 1991 Mount Unzen mixed magma. *J. Volcanol. Geotherm. Res.* **89**, 213–230 (1999).
33. Koleszar, A. M., Kent, A. J. R., Wallace, P. J. & Scott, W. E. Controls on long-term low explosivity at andesitic arc volcanoes: insights from Mount Hood, Oregon. *J. Volcanol. Geotherm. Res.* **219-220**, 1–14 (2012).
34. Degruyter, W., Huber, C., Bachmann, O., Cooper, K. M. & Kent, A. J. R. Influence of exsolved volatiles on reheating silicic magmas by recharge and consequences for eruptive style at Volcan Quizapu (Chile). *Geochem. Geophys. Geosyst.* **18**, 4123–4135 (2017).
35. Popa, R.-G. et al. A connection between magma chamber processes and eruptive styles revealed at Nisyros-Yali volcano (Greece). *J. Volcanol. Geotherm. Res.* **387**, 106666 (2019).
36. Zhang, Y., Stolper, E. M. & Wasserburg, G. J. Diffusion of water in rhyolitic glasses. *Geochim. Cosmochim. Acta* **55**, 441–456 (1991).
37. Severs, M. J., Azbej, T., Thomas, J. B., Mandeville, C. W. & Bodnar, R. J. Experimental determination of H_2O loss from melt inclusions during laboratory heating: evidence from Raman spectroscopy. *Chem. Geol.* **237**, 358–371 (2007).
38. Waters, L. E. & Lange, R. A. An updated calibration of the plagioclase-liquid hygrometer-thermometer applicable to basalts through rhyolites. *Am. Mineral.* **100**, 2172–2184 (2015).
39. Edmonds, M. & Woods, A. W. Exsolved volatiles in magma reservoirs. *J. Volcanol. Geotherm. Res.* **368**, 13–30 (2018).
40. Gualda, G. A. R., Ghiorso, M. S., Lemons, R. V. & Carley, T. L. Rhyolite-MELTS: A modified calibration of MELTS optimized for silica-rich, fluid-bearing magmatic systems. *J. Petrol.* **53**, 875–890 (2012).
41. Huppert, H. E. & Woods, A. W. The role of volatiles in magma chamber dynamics. *Nature* **420**, 493–495 (2002).
42. Mastin, L. G., Roeloffs, E., Beeler, N. M. & Quick, J. E. *Constraints on the size, overpressure, and volatile content of the Mount St. Helens magma system from geodetic and dome-growth measurements during the 2004–2006+ eruption* Professional Paper 1750; 461–488 (USGS, 2008).
43. Popa, R.-G. et al. Water exsolution in the magma chamber favors effusive eruptions: application of Cl-F partitioning behavior at the Nisyros–Yali volcanic area. *Chem. Geol.* **570**, 120170 (2021).
44. Newman, S. & Lowenstern, J. B. VolatileCalc: a silicate melt-H_2O-CO_2 solution model written in Visual Basic for Excel. *Comput. Geosci.* **28**, 597–604 (2002).
45. Spieler, O. et al. The fragmentation threshold of pyroclastic rocks. *Earth Planet. Sci. Lett.* **226**, 139–148 (2004).
46. Zhang, Y. A criterion for the fragmentation of bubbly magma based on brittle failure theory. *Nature* **402**, 648–650 (1999).
47. Gonnermann, H. & Manga, M. Explosive volcanism may not be an inevitable consequence of magma fragmentation. *Nature* **426**, 432–435 (2003).
48. Alidibirov, M. & Dingwell, D. B. Magma fragmentation by rapid decompression. *Nature* **380**, 146–148 (1996).
49. Pistone, M., Caricchi, L. & Ulmer, P. CO_2 favours the accumulation of excess fluids in felsic magmas. *Terra Nova* **33**, 120–128 (2020).
50. Oppenheimer, J., Rust, A. C., Cashman, K. V. & Sandnes, B. Gas migration regimes and outgassing in particle-rich suspensions. *Front. Phys.* **3**, 60 (2015).
51. Parmigiani, A., Degruyter, W., Leclaire, S., Huber, C. & Bachmann, O. The mechanics of shallow magma reservoir outgassing. *Geochem. Geophys. Geosyst.* **18**, 2887–2905 (2017).
52. Colombier, M. et al. In situ observation of the percolation threshold in multiphase magma analogues. *Bull. Volcanol.* **82**, 32 (2020).
53. Popa, R.-G., Dietrich, V. J. & Bachmann, O. Effusive–explosive transitions of water-undersaturated magmas. The case study of Methana volcano, South Aegean Arc. *J. Volcanol. Geotherm. Res.* **399**, 106884 (2020).
54. Hess, K.-U. & Dingwell, D. B. Viscosities of hydrous leucogranitic melts: a non-Arrhenian model. *Am. Mineral.* **81**, 1297–1300 (1996).
55. Degruyter, W. & Huber, C. A model for eruption frequency of upper crustal silicic magma chambers. *Earth Planet. Sci. Lett.* **403**, 117–130 (2014).
56. Townsend, M., Huber, C., Degruyter, W. & Bachmann, O. Magma chamber growth during intercaldera periods: insights from thermo-mechanical modeling with applications to Laguna del Maule, Campi Flegrei, Santorini, and Aso. *Geochem. Geophys. Geosyst.* **20**, 1574–1591 (2019).
57. Kozono, T. et al. Magma discharge variations during the 2011 eruptions of Shinmoe-dake volcano, Japan, revealed by geodetic and satellite observations. *Bull. Volcanol.* **75**, 695 (2013).
58. Hill, G. J. et al. Temporal magnetotellurics reveals mechanics of the 2012 Mount Tongariro, NZ, Eruption. *Geophys. Res. Lett.* **47**, e2019GL086429 (2019).
59. Marsh, B. D. On the crystallinity, probability of occurrence, and rheology of lava and magma. *Contrib. Mineral. Petrol.* **78**, 85–98 (1981).

Publisher's note Springer Nature remains neutral with regard to jurisdictional claims in published maps and institutional affiliations.

Data availability

The excel source file containing the geochemical and petrological data the meta-analysis is based on can be retrieved from the EarthChem data repository, at https://doi.org/10.26022/IEDA/112061, under the title 'Global overview of pre-eruptive magma chamber conditions'[60]. The source files containing the results of the numerical simulations[61] can be retrieved from EarthChem, at https://doi.org/10.26022/IEDA/112064. Source data are provided with this paper.

References

60. Popa, R.-G., Bachmann, O. & Huber, C. Global overview of pre-eruptive magma chamber conditions, version 1.0. EarthChem https://doi.org/10.26022/IEDA/112061 (2021).
61. Popa, R.-G., Bachmann, O. & Huber, C. Source data for "Explosive or effusive style of volcanic eruption determined by magma storage conditions," version 1.0. EarthChem https://doi.org/10.26022/IEDA/112064 (2021).

Acknowledgements

O.B. acknowledges funding from the Swiss National Science Foundation grant 200021_178928 and C.H. from National Science Foundation fund EAR-20211328. The funders had no role in study design, data collection and analysis, decision to publish or preparation of the manuscript.

Author contributions

R.-G.P and O.B. conceptualized the study. R.-G.P. collected the global dataset and performed the calculations for the pre-eruptive magma chamber conditions. O.B. performed the calculations for the evolution of the volume of exsolved volatiles with crystallization. C.H. performed the calculations estimating the effect of exsolved volatiles upon magma recharge in the subvolcanic storage region. R.-G.P. drafted the manuscript together with O.B. and C.H. All authors contributed to the interpretation of the results and to the preparation of the manuscript.

Competing interests

The authors declare no competing interests.

Additional information

Supplementary information The online version contains supplementary material available at https://doi.org/10.1038/s41561-021-00827-9.

Correspondence and requests for materials should be addressed to Răzvan-Gabriel Popa.

Peer review information Primary Handling editor: Rebecca Neely, in collaboration with the *Nature Geoscience* team. *Nature Geoscience* thanks Takehiro Koyaguchi, Edward Llewellin and the other, anonymous, reviewer(s) for their contribution to the peer review of this work.